

Incorporation and Replication of 8-Oxo-deoxyguanosine by the Human Mitochondrial DNA Polymerase*

Received for publication, August 21, 2006, and in revised form, September 27, 2006. Published, JBC Papers in Press, September 27, 2006, DOI 10.1074/jbc.M607965200

Jeremiah W. Hanes, David M. Thal, and Kenneth A. Johnson¹

From the Department of Chemistry and Biochemistry, Institute for Cellular and Molecular Biology, The University of Texas, Austin, Texas 78712

To assess the role of oxidative stress on the replication of mitochondrial DNA, we examined the kinetics of incorporation of 8-oxo-7,8-dihydroguanosine (8-oxodG) triphosphate catalyzed by the human mitochondrial DNA polymerase. Using transient state kinetic methods, we quantified the kinetics of incorporation, excision, and extension beyond a base pair containing 8-oxodG. The 8-oxodGTP was incorporated opposite dC in the template with a specificity constant of $0.005 \mu\text{M}^{-1} \text{s}^{-1}$, a value $\sim 10,000$ -fold lower than that for dGTP. Once incorporated, 96% of the time 8-oxodGMP was extended by continued polymerization rather than being excised by the proofreading exonuclease. The specificity constant for incorporation of 8-oxodGTP opposite a template dA was $0.2 \mu\text{M}^{-1} \text{s}^{-1}$, a value 13-fold higher than incorporation opposite a template dC. The 8-oxodG:dA mismatch was extended rather than excised at least 70% of the time. Examination of the kinetics of polymerization with 8-oxodG in the template strand also revealed relatively low fidelity in that dCTP would be incorporated only 90% of the time. In nearly 10% of events, dATP would be incorporated, and once incorporated dA (opposite 8-oxodG) was extended rather than excised. The greatest fidelity was against a dTTP:8-oxodG mismatch affording a discrimination value of only 1800. These data reveal that 8-oxodGTP is a potent mutagen. Once it is incorporated into DNA, 8-oxodGMP codes for error prone DNA synthesis. These reactions are likely to play important roles in oxidative stress in mitochondria related to aging and as compounded by nucleoside analogs used to treat human immunodeficiency virus infections.

Although many theories exist regarding the underlying molecular mechanisms behind aging in mammals, it is clear that mitochondrial integrity plays a major role (1–3). According to the free radical theory of aging, electrons from the electron transport chain are able to reduce molecular oxygen to form superoxide anion radicals (O_2^-) during aerobic respiration. These reactive radicals go on to produce

other reactive oxygen species (ROS)² (3). ROS can be generated at a few cellular sites, but in healthy tissues the majority are a result of aerobic metabolism, and consequently, they are always present during normal cellular activity. ROS attack a variety of different cellular macromolecules, including proteins, lipids, and DNA. However, damage to mitochondrial DNA (mtDNA) has been implicated as important in regard to aging, especially in postmitotic cells, such as neurons (4). A cycle is created in the mitochondria in which a continued state of oxidative stress leads to further damage to electron transport chain components, ultimately causing an energy decline, carcinogenesis, and many age-related diseases (5).

One of the most common products of oxidative DNA damage is 8-oxo-7,8-dihydroguanosine (8-oxodG), which is reported to be highly mutagenic and is commonly used as biomarker for oxidative stress. Basal levels of 8-oxodG in mtDNA between different species correlate negatively with longevity in many mammals and birds, which is not the case with nuclear DNA (6). Moreover, because of the proximity of mtDNA to the electron transport chain, the levels of oxidative damage are significantly higher than in the nucleus in all tissues of mammals and birds examined (7).

The repair of 8-oxodG in the mitochondria is carried out by the base excision repair pathway, and its efficiency can be evaluated by 8-oxodG glycosylase activity, which increases over the life span of rodents but does not seem to stop the accumulation of 8-oxodG during aging (8, 9). In addition to the direct damage of mtDNA by ROS, free nucleotides can be damaged and may compete with undamaged nucleotides during replication to increase the rate of mutation (for review, see Ref. 10). Humans encode a triphosphatase termed MutT homolog-1 that is able to alleviate the mutagenic effects of 8-oxodGTP by hydrolyzing it to 8-oxodGMP, thus reducing the occurrence of A to C transversions (11). This enzyme has been shown to be present in the cytosol and the mitochondria (12, 13), although in general, the mitochondrial DNA damage repair systems are relatively simple and limited compared with those in the nucleus (14).

The concern surrounding 8-oxodG stems from its mutagenic coding potential when copied by an assortment of mammalian and prokaryotic polymerases (10, 15–18). For all studies done with DNA polymerases, dCMP and dAMP were

* This work was supported by National Institutes of Health Grant R01 GM044613 and the Welch Foundation Grant F-1604. The costs of publication of this article were defrayed in part by the payment of page charges. This article must therefore be hereby marked "advertisement" in accordance with 18 U.S.C. Section 1734 solely to indicate this fact.

¹ To whom correspondence should be addressed: Institute for Cellular and Molecular Biology, University of Texas at Austin, 2500 Speedway, A4800, Austin, TX 78735. Tel.: 512-471-0434; Fax: 512-471-0435; E-mail: kajohnson@mail.utexas.edu.

² The abbreviations used are: ROS, reactive oxygen species; 8-oxodG, 8-oxo-7,8-dihydroguanosine; Pol γ , human mitochondrial DNA polymerase holoenzyme.

Incorporation of 8-Oxo-dGTP by Pol γ

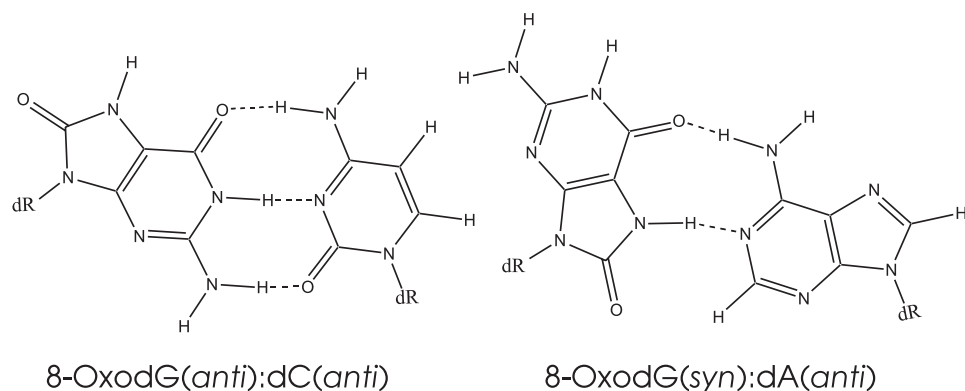


FIGURE 1. **Base-pairing conformations of 8-oxodG.** Shown on the *left* is a normal Watson-Crick hydrogen bonding arrangement between 8-oxodGMP and dCMP in which both 8-oxodG and dCMP are in the *anti* conformation. Shown on the *right* is the Hoogsteen base pair of 8-oxodG and dAMP in which 8-oxodG is rotated to the *syn* conformation. The was adapted from Krahn *et al.* (20).

inserted across from 8-oxodGMP with comparable but varying efficiencies, which potentially results in a G to T transversion mutation. The molecular mechanism for the lack of specificity afforded by 8-oxodGMP is thought to be due to its ability to form either a normal Watson-Crick hydrogen-bonding arrangement with dCMP or a Hoogsteen base pair with dAMP by flipping to the *syn* conformation as depicted in Fig. 1 (19, 20).

Arguably, the most important polymerase in regard to the replication of oxidatively damaged DNA is the human mitochondrial polymerase γ (Pol γ), which is solely responsible for the propagation of the mitochondrial genome. Mice expressing a homozygous knock-in mutant of a proofreading-deficient version of Pol γ prematurely developed numerous signs of aging (21). A more recent study using a similar mouse model also showed that the integrity of the mitochondrial genome was important in the development of premature signs of aging. However, this study found no increase in the levels of ROS as the amount of mtDNA mutations increased (22). Interestingly, a different approach aimed at directly assessing the role of ROS on aging in another transgenic mouse model was undertaken in which human catalase was expressed and localized to the mitochondria and shown to extend maximum life span (23).

Taken together, the available information pertaining to the molecular mechanisms of aging seems to implicate the integrity of the mitochondrial genome as an important factor. Specifically, it appears that the accumulation of mutations in the mtDNA appears to have a deleterious effect on metabolism and maximum life span. In addition, the toxic side effects of nucleoside analogs used to treat viral infections, although due primarily to inhibition of mitochondrial DNA replication (24), are compounded by the resulting, accumulative oxidative stress (25). We, therefore, sought to clearly define the role of 8-oxodG in mitochondrial DNA replication by means of transient state kinetic methods using recombinant human Pol γ holoenzyme and defined oligonucleotide primer/template combinations. Most strikingly, our results show that the free damaged nucleotide is incorporated efficiently opposite dA, and the polymerase efficiently

extends the primer to bury the 8-oxodG:dA mismatch. Once in the template strand, 8-oxodG is a potent mutagen.

MATERIALS AND METHODS

Nucleotides and Oligonucleotides—The nucleotide, 8-oxodGTP, was purchased from TriLink BioTechnologies (San Diego, CA), and unmodified dNTPs were purchased from Sigma-Aldrich. Oligonucleotides containing 8-oxodGMP (except for a primer 3'-terminated with 8-oxodGMP) were purchased from The Midland Certified Reagent Co. (Midland, TX). All other oligonucleotides were purchased

from Integrated DNA Technologies (Coralville, IA).

Pol γ Expression and Purification—Overexpression and purification of recombinant human Pol γ were previously described (26, 27). Holoenzyme was reconstituted at a 1:5 ratio of catalytic subunit to accessory subunit. Forward polymerization studies were conducted using an exonuclease-deficient mutant (E200A).

Preparation of DNA—Studies were carried out using synthetic oligonucleotide primers and templates. The primers varied in length from 24 to 27 nucleotides, whereas the template was always 45 bases long. The general 25-mer primer sequence was 5'-GCCTCGCAGCCGTCACCAACTCA-3', and the 45-mer template sequence was 5'-GGACGGCATTGGATC-GACAXT**GAGTTGGTTGGACGGCTGCGAGGC**-3', where the boldface, italic *X* in the template was 8-oxodGMP, dAMP, or dCMP. Specific sequence changes to the general primer and template sequences given above are detailed under "Results" and in the figures. For example, replacement of template base *X* is designated as 45C-mer (Fig. 4). The primers were 5'-³²P-labeled using T4 polynucleotide kinase, according to the manufacturer's instructions (Invitrogen). The reaction was terminated by incubation at 95 °C for 5 min, and excess nucleotide was removed using a Bio-Spin 6 column (Bio-Rad). The primer was annealed to 45-mer template by combining at an equimolar ratio, heating to 95 °C, and slowly cooling to room temperature. Primers containing 3'-terminal 8-oxodGMP were enzymatically synthesized as follows. A single nucleotide incorporation reaction was performed using 1 μ M Pol γ holoenzyme (E200A), 100 μ M duplex DNA (containing dC as the template base opposite 26th primer position), and 150 μ M 8-oxodGTP in 50 mM Tris-Cl, pH 7.5, 100 mM NaCl, 2.5 mM MgCl₂. The reaction mixture was incubated at 37 °C for 30 min, and then the product was gel-purified to obtain the 8-oxodGMP-terminated primer. Primer was labeled with ³²P on the 5'-end, and DNA duplex was annealed as described above.

Polymerization and Exonuclease Reaction Conditions—For reactions too fast to measure by manual mixing and quenching, a quench-flow apparatus (RFQ-3) from KinTek Corp. was used. All incorporation assays were performed at 37 °C in buffer containing 50 mM Tris-Cl, pH 7.5, 100 mM NaCl, and 2.5 mM

$$\% \text{ Buried} = \frac{k_{\text{pol}}}{k_{\text{pol}} + k_{\text{exo}}} \times 100 \quad (\text{Eq. 5})$$

MgCl₂. The holoenzyme was reconstituted by incubating the two protein subunits for 5 min on ice in reaction buffer lacking magnesium. The DNA duplex was then added, and the mixture was incubated for an additional 5 min on ice. Incorporation reactions were initiated by the addition of nucleotide and magnesium in the same reaction buffer at 37 °C and then quenched with 0.5 M EDTA. Alternatively, the excision reactions were initiated by the addition of 2.5 mM MgCl₂ and quenched in the same fashion as the polymerization reactions. Previous work on T7 DNA polymerase has shown that the addition of Mg²⁺ leads to a faster reaction than observed by initiating the reaction by mixing enzyme with DNA (28, 29). Therefore, this method provides the best estimate of the intrinsic rates of reaction, and it is unlikely that our measurements are limited by the rate of Mg²⁺ binding. All concentrations refer to the final post-mixing reaction conditions. Substrates were separated from products by 15% denaturing polyacrylamide sequencing gels (PAGE), imaged on a GE Healthcare Storm 860 Imager, and quantified using ImageQuant software (Amersham Biosciences).

Data Analysis—Single nucleotide incorporation assays were performed using varying concentrations of dNTP to examine the nucleotide concentration dependence of the incorporation rate or amplitude. Single-turnover conditions were employed in which the concentration of enzyme was greater than the concentration of DNA substrate. Specific reaction conditions are listed in each figure legend. A time course was performed for each concentration of dNTP. To normalize data, the integrated volume of product (DNA_{n+1}) was divided by the sum of the substrate and product volumes (DNA_n + DNA_{n+1}) and multiplied by the concentration of DNA used in the experiment. The concentration of extended DNA product was plotted against time (*t*) and fit to a single (Equation 1) or double exponential equation (Equation 2). All nonlinear regression analysis was performed in the program GraFit 5 (Erithacus Software, Horley Surrey, UK).

$$[\text{Product}] = A_1 e^{-k_1 t} + C \quad (\text{Eq. 1})$$

$$[\text{Product}] = A_1 e^{-k_1 t} + A_2 e^{-k_2 t} + C \quad (\text{Eq. 2})$$

The observed reaction rates (*k*₁ and/or *k*₂) and in one case the amplitudes (*A*₁ and/or *A*₂) were plotted against dNTP concentration, and the data were fit to a hyperbola.

$$k_{\text{obs}} = \frac{k_{\text{pol}}[\text{dNTP}]}{K_d + [\text{dNTP}]} \quad (\text{Eq. 3})$$

$$A_{\text{obs}} = \frac{A_{\text{max}}[\text{dNTP}]}{K_d + [\text{dNTP}]} \quad (\text{Eq. 4})$$

In the above equations *K*_d is the apparent ground state dissociation constant, *k*_{pol} is the maximum rate of polymerization, *A*_{obs} is the observed amplitude, and *A*_{max} is defined as the maximum amplitude at infinite nucleotide concentration. The percent probability of nucleotide extension *versus* exonuclease removal (or percent buried) was calculated using the maximum rate of polymerization (*k*_{pol}), and the rate of exonuclease removal (*k*_{exo}) according to the following equation.

Simulation—The program KinTekSim (KinTek Corp.) was used for kinetic simulation of experimental data. The simulation was refined by an iterative process until a “best fit” was obtained according to the mechanism described under “Results.” The simulated curves were then exported from KinTekSim and plotted with the raw data in the program GraFit 5.

RESULTS

“Correct” Incorporation of 8-OxodGTP—To assess the physiological relevance of 8-oxodGTP on the overall fidelity of mitochondrial DNA replication, we inspected its incorporation by reconstituted exonuclease-deficient human Pol γ holoenzyme using a defined primer/template combination of 25 and 45 bases, respectively (see under “Materials and Methods”). The template was modified at the position across from the incoming nucleotide to be either dCMP or dAMP. The terminology used in this report will refer to 8-oxodGTP incorporation across from a template dCMP as correct and across from a template dAMP as “incorrect.” Only 8-oxodGTP was present during the incorporation reaction so that the primer would be extended by only one nucleotide to simplify data analysis and interpretation. The primer extension reactions were performed under single turnover conditions ([enzyme] > [DNA]) to circumvent the complications that arise from multiple turnovers with processive enzymes. A series of experiments was performed at various 8-oxodGTP concentrations to obtain the concentration dependence of the rate and amplitude of incorporation. For typical correct incorporation reactions under these conditions the concentration dependence of the rate of incorporation defines the ground state nucleotide dissociation constant or *K*_d and the maximum rate of incorporation or *k*_{pol}. Additionally, because nucleotide binding rapidly comes to equilibrium (relative to the rate of incorporation) and is followed by a single rate-limiting step, the *k*_{pol} and *K*_d are equal to the *k*_{cat} and *K*_m, respectively. As a consequence, the ratio, *k*_{pol}/*K*_d defines the specificity constant (*k*_{cat}/*K*_m) for incorporation.

In this context we refer to the theoretical values of *k*_{cat} and *K*_m that might be derived during processive DNA synthesis and not the artificially low and inaccurate values that are experimentally obtained in steady state measurements of single nucleotide incorporation, limited by the release of DNA from the enzyme. As discussed in the accompanying paper (30) and elsewhere (28, 31, 32), measurements of *k*_{pol} and *K*_d in rapid quench experiments provide the best estimate for nucleotide selectivity.

Incorporation reactions were initiated by rapidly mixing the preformed holoenzyme-DNA complex with 8-oxodGTP and Mg²⁺. Then, after various times the reactions were quenched with 0.5 M EDTA. The time dependence of the correct incorporation of 8-oxodGTP onto a template dCMP is shown in Fig. 2A. Unexpectedly, the extension reaction proceeded in a biphasic fashion, and therefore, the data were fit by nonlinear regression to a double exponential equation (Equation 2). The most obvious nucleotide concentration dependence of incorporation was the amplitude of the fast phase of the reaction and is shown

Incorporation of 8-Oxo-dGTP by Pol γ

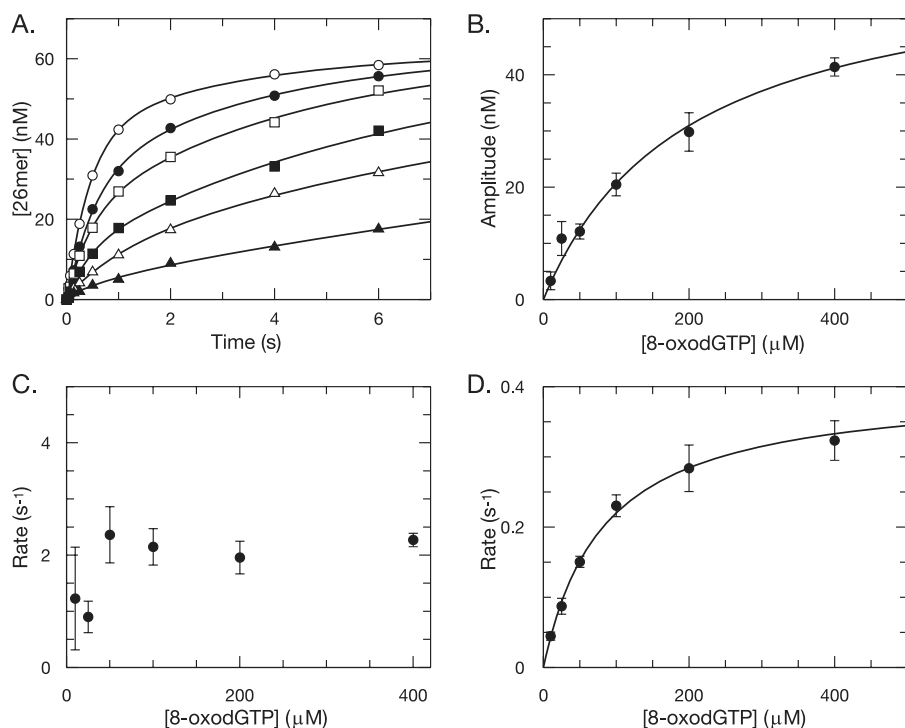


FIGURE 2. **Incorporation of 8-oxodGTP onto dCMP.** A, 100 nM exonuclease-deficient holoenzyme was preincubated with 90 nM 25/45-mer (G incorporation) DNA duplex and then rapidly mixed with Mg^{2+} and various concentrations of 8-oxodGTP (10 (\blacktriangle), 25 (\triangle), 50 (\blacksquare), 100 (\square), 200 (\bullet), and 400 (\circ) μ M). Each data set was fit by nonlinear regression to a double exponential equation (Equation 2) to obtain the rates and amplitudes of incorporation. B, the amplitudes of the fast phase were plotted as a function of 8-oxodGTP concentration. A fit of the data to a hyperbola (Equation 4) yields an apparent $K_d = 200 \pm 30 \mu$ M and an A_{max} (maximum amplitude) = 62 ± 4 nM. C, the rate from the fast phase of each reaction was plotted as a function 8-oxodGTP concentration to show that the rate of the initial fast phase is not clearly dependent upon the concentration of 8-oxodGTP. D, the rate from the slow phase of each reaction was plotted as a function of 8-oxodGTP concentration and fit to a hyperbola (Equation 3) to yield an apparent $K_d = 83 \pm 7 \mu$ M and a $k_{max} = 0.4 \pm 0.02 s^{-1}$.

in Fig. 2B. The amplitude appeared to saturate in a hyperbolic fashion as a function of 8-oxodGTP concentration and was fit by nonlinear regression to a hyperbola (Equation 4) defining a maximum amplitude (A_{max}) of 62 ± 4 nM and an apparent K_d of $200 \pm 30 \mu$ M. A plot of the rate of incorporation for the same phase (Fig. 2C) reveals that there is no clear dependence on the concentration of nucleotide. If one simply looks at the concentration dependence of the fast phase of the reaction, it appears that ground state nucleotide binding is reversibly linked to bond formation between 8-oxodGMP and the primer strand. However, one further complication is illustrated in Fig. 2D, where the rate of the slow phase is plotted as a function of 8-oxodGTP concentration. It also saturates with high concentrations of 8-oxodGTP. The data were fit to a hyperbola (Equation 3) defining a maximum rate of $0.4 \pm 0.02 s^{-1}$ and an apparent K_d of $83 \pm 7 \mu$ M. These data suggest that the chemistry step is reversibly linked to nucleotide binding and that the release of pyrophosphate from the active site is relatively slow and is limited by the isomerization of the polymerase after primer extension. The possibility that the enzyme remains in a closed conformation after the chemistry step would explain the fact that the amplitude of the fast phase is dependent on the concentration of 8-oxodGTP in solution because the active site residues responsible for catalysis would still be in alignment to perform the reverse reaction. But once the enzyme undergoes a conformational change and releases pyrophosphate, the reaction

would precede to a common end point as a function of the rate of that isomerization step. To illustrate this we performed a kinetic simulation using the program KinTekSim (Fig. 3A) using a simple three-step mechanism (Fig. 3B). The curves that are superimposed with the raw data were generated by an iterative process using the kinetic parameters obtained by nonlinear regression as an initial guide. The final best-fit rate constants are shown with the mechanism used. An initial collision of 8-oxodGTP with the *E*-DNA complex fits best with a true K_d of about 135μ M. Next, the chemistry step follows at a rate of about $2 s^{-1}$ ($k_{forward}$) and is reversible at a rate of about $0.7 s^{-1}$ ($k_{reverse}$). It is not known if a conformational change limits the rate of the chemistry step. After the chemistry step, the release of pyrophosphate ($\sim 0.4 s^{-1}$) limits the net rate of incorporation. It is reasonable to suppose that a conformational change defines the rate of pyrophosphate dissociation, but we have no evidence to address this issue. Pyrophosphate release is essentially irreversible because of the relatively low concentration of

PP_i formed during the course of the reaction.

The pathway and rate constants shown in Fig. 3B define a specificity constant of 0.005μ M⁻¹ s⁻¹ computed from $k_{cat}/K_m \sim k_2k_3/(K_d(k_{-2} + k_3))$ where the steps are numbered sequentially, and $K_d = 135 \mu$ M represents the ground stand dissociation constant. This specificity constant is $\sim 10,000$ -fold lower than the value for correct incorporation (50μ M⁻¹ s⁻¹). Interestingly, the slow pyrophosphate release rate allows the chemistry step to come to equilibrium with dNTP binding, thereby explaining the concentration dependence of the amplitude of incorporation, whereas the rate is nearly constant. In addition, this effect reduces k_{cat}/K_m .

Exonuclease Removal of 8-oxodGMP—The overall fidelity of replication with respect to 8-oxodG will depend on not only the rate of incorporation but also on the rate of removal once incorporated. To measure the rate of removal, a primer strand 3'-terminated with the damaged base needed to be synthesized. This was accomplished enzymatically and is detailed under "Materials and Methods." The primer strand was annealed to a complementary template (dCMP across from 8-oxodGMP at the 26th position) and then preincubated with wild type Pol γ holoenzyme in the absence of Mg^{2+} . To start the reaction an equal volume of buffer containing Mg^{2+} was rapidly mixed with the *E*-DNA complex and quenched with EDTA as described for the incorporation reactions. The time dependence of the removal of 8-oxodGMP is shown in Fig. 4, plotted as the con-

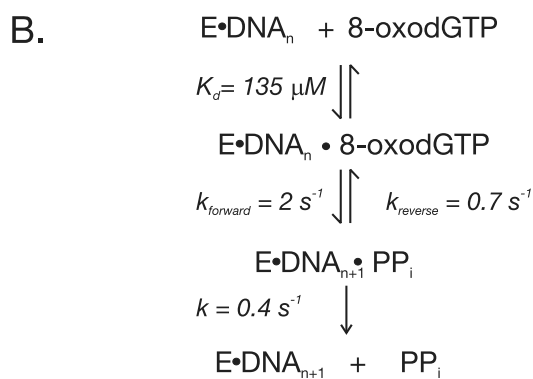
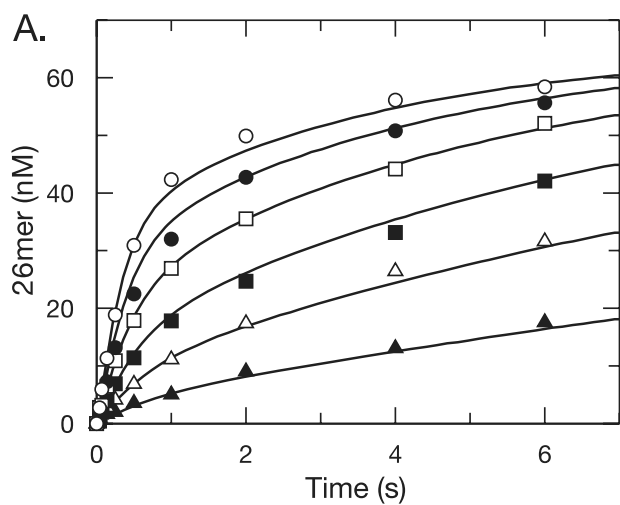


FIGURE 3. **Global fitting of 8-oxodGTP incorporation.** A, shown are the experimentally obtained data for the incorporation of 8-oxodGTP onto a template dCMP. The curves superimposed with the experimental data were generated using the program KinTekSim by iterative global fitting to all the data using the kinetic mechanism and rates shown in the scheme (B).

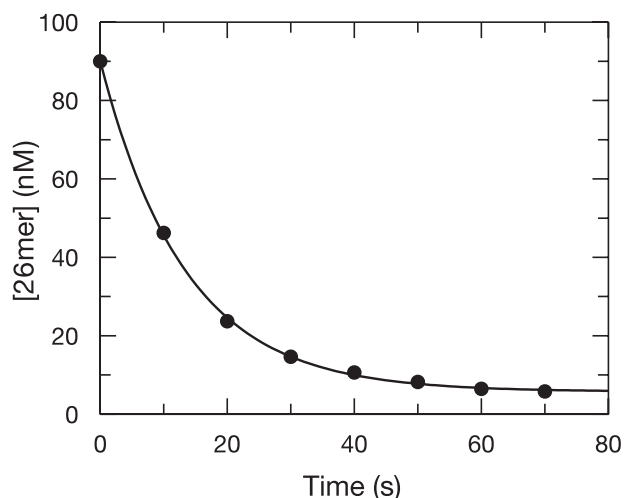


FIGURE 4. **Exonuclease removal of 8-oxodGMP-based paired with dCMP.** Wild type holoenzyme (100 nM) was preincubated with 90 nM 26(8-oxodG)/45C-mer DNA duplex and mixed with Mg^{2+} to start the reaction. The concentration of substrate was plotted as a function of time and fit to a single exponential equation (Equation 1) to obtain a k_{exo} of $0.075 \pm 0.002 \text{ s}^{-1}$ with an amplitude of $84.4 \pm 0.7 \text{ nM}$.

concentration of substrate 26-mer remaining *versus* time. The data were fit by nonlinear regression to a single exponential equation (Equation 1) to obtain a k_{exo} of $0.075 \pm 0.002 \text{ s}^{-1}$.

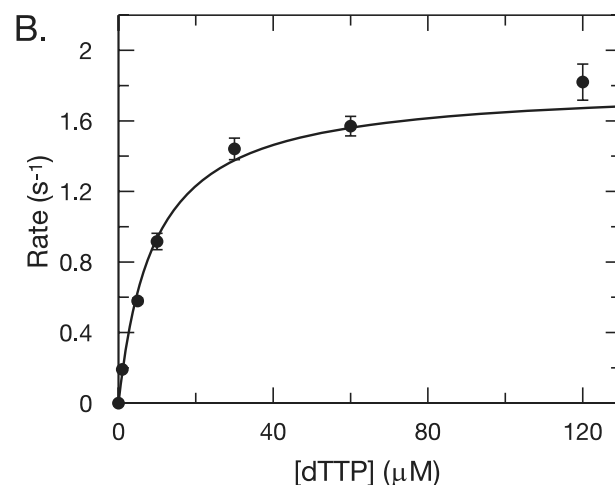
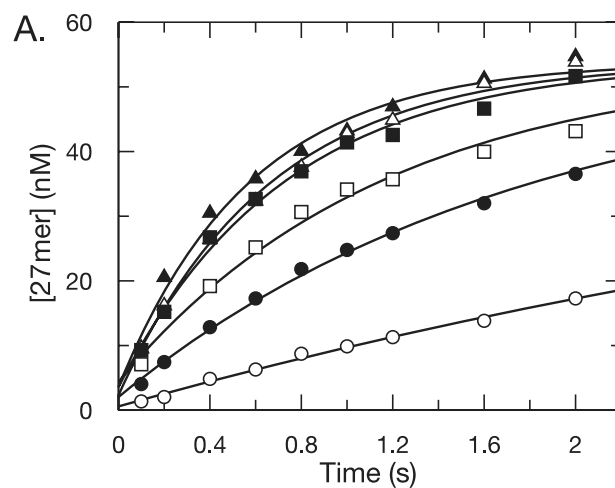


FIGURE 5. **Correct incorporation of dTTP onto a primer terminated with 8-oxodGMP.** A, 100 nM exonuclease-deficient holoenzyme was preincubated with 90 nM 26(8-oxodG)/45CA-mer DNA duplex and then rapidly mixed with Mg^{2+} and various concentrations of dTTP (1 (○), 5 (●), 10 (□), 30 (■), 60 (△), and 120 (▲) μM). Each data set was fit by nonlinear regression to a single exponential equation to obtain the rate of incorporation. B, the observed rates were plotted as a function of dTTP concentration. A fit of the data to a hyperbola yielded a $K_d = 9.3 \pm 1.0 \mu\text{M}$ and a $k_{\text{pol}} = 1.8 \pm 0.1 \text{ s}^{-1}$.

Probability of Extension—The probability of extension to bury a misincorporated or damaged base pair depends on the relative rate of removal *versus* the rate of incorporation of the next correct base pair. Therefore, we examined kinetic parameters for the incorporation of dTTP (next correct base pair after an 8-oxodG:dC base pair). The experiment was performed in a manner identical to that of 8-oxodGTP, and the results are shown in Fig. 5A. The time dependence of incorporation followed a single exponential rise, and the rates of incorporation saturated hyperbolically to define a k_{pol} of $1.8 \pm 0.1 \text{ s}^{-1}$ and a K_d of $9.3 \pm 1.0 \mu\text{M}$. Comparing the k_{pol} of 1.8 s^{-1} to the k_{exo} of 0.075 s^{-1} for 8-oxodGMP predicts that the probability of burial is about 96% (Equation 5). However, if the physiological concentrations of dTTP in the mitochondria are as low as $1 \mu\text{M}$, as has been estimated (33), then the probability of extension *versus* excision would be 70%. Although the physiological concentrations of dTTP in the mitochondria are not known with certainty, it appears that 8-oxodGMP, once incorporated, is most often buried rather than excised.

Incorporation of 8-Oxo-dGTP by Pol γ

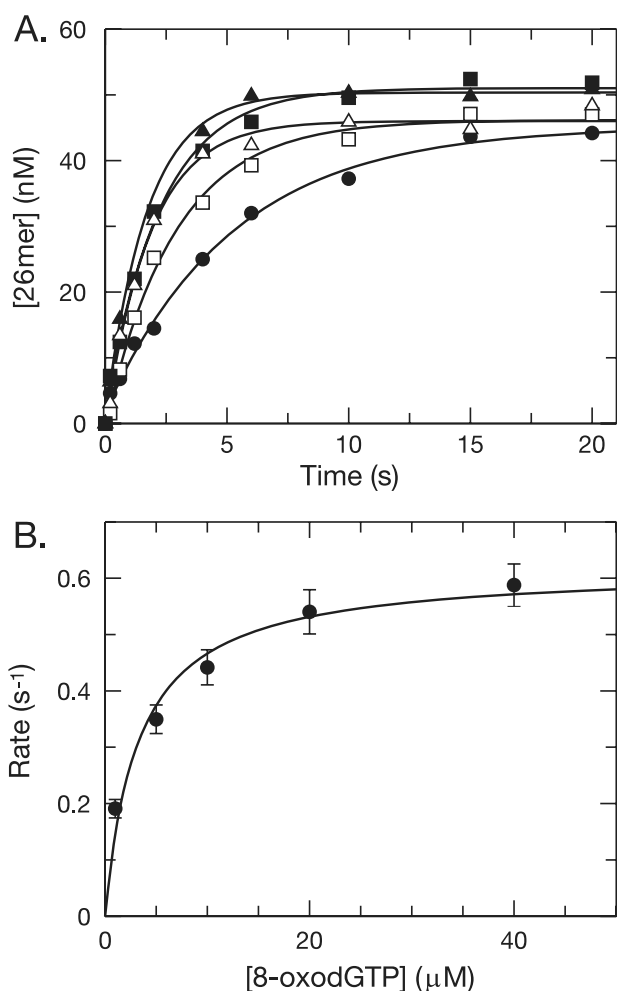


FIGURE 6. **Incorporation of 8-oxodGTP onto dAMP.** *A*, exonuclease-deficient holoenzyme (100 nM) was preincubated with 90 nM 25/45CA-mer DNA duplex and then rapidly mixed with Mg^{2+} and various concentrations of 8-oxodGTP (1 (●), 5 (□), 10 (■), 20 (△), and 40 (▲) μM). Each data set was fit by nonlinear regression to a single exponential equation to obtain the rate of incorporation. *B*, the observed rates were plotted as a function of 8-oxodGTP concentration and fit to the hyperbola to yield a $K_d = 3.3 \pm 1.0 \mu M$ and a $k_{pol} = 0.62 \pm 0.05 s^{-1}$.

Incorrect Incorporation of 8-OxodGTP—Because of the possibility that the formation a Hoogsteen base pair between an incoming 8-oxodGTP and a template dAMP might lead to relatively efficient incorporation, we inspected the kinetic parameters governing this process. Shown in Fig. 6A is the time dependence of primer extension performed at several concentrations of 8-oxodGTP. The data were best fit to a single exponential equation, and the rate of incorporation saturated in a hyperbolic fashion as a function of concentration (Fig. 6B) defining a k_{pol} of $0.62 \pm 0.05 s^{-1}$ and a K_d of $3.3 \pm 1.0 \mu M$ to yield an overall specificity constant of $0.187 \pm 0.0586 \mu M^{-1} s^{-1}$. To our surprise, 8-oxodGTP is a 12.5-fold better substrate for incorporation across from dAMP compared with dCMP. Because of this result, it was important to define the probability of burial of this mutagenic base pair by measuring the rate of removal and the kinetic parameters for the next correct incorporation (results not shown). All the results examining polymerization with regard to the incorporation of 8-oxodGTP (correct and incorrect) are shown in Fig. 7 as will be detailed under “Discussion.”

Fidelity of Polymerization with 8-OxodGMP in the Template Strand—Because no detailed studies have been reported for the fidelity of the replication of oxidatively damaged DNA using the human mitochondrial polymerase, we performed a series of single turnover experiments examining the incorporation and removal of nucleotides before, onto, and beyond an 8-oxodGMP in the template strand. In all cases the incorporation data were easily explained by a rapid equilibrium binding model, where the observed rate of polymerization saturated hyperbolically, defining the kinetic parameters for incorporation. The removal of each nucleotide was also inspected so that the probability of extension *versus* excision could be calculated as summarized in Fig. 8. The data for the two most probable replication routes are depicted as a side-by-side comparison and are referred to as correct and incorrect pathways. The correct pathway refers to the incorporation of dCTP onto a template 8-oxodGMP, and the incorrect pathway refers to dATP incorporation. Table 1 was constructed to compare our results for the incorporation of all four nucleotides onto a template 8-oxodGMP.

It is clear from the data summarized in Fig. 8 that once dCTP or dATP is incorporated opposite 8-oxodG, the polymerization reaction continues to “bury” either 8-oxodG:dNTP base pair. Although the specificity constants for the subsequent incorporations of dTTP and dGTP are reduced somewhat from those seen with a normal primer/template, the rates of excision by the 3′-5′ exonuclease are not sufficiently fast relative to the rates of extension to contribute to fidelity. Thus, there is no proofreading of errors opposite 8-oxodG.

DISCUSSION

One of the most important results of this report is the significant preference for 8-oxodGTP incorporation onto a template dAMP rather than dCMP. To quantify the likelihood of misincorporation, the discrimination against 8-oxodGTP *versus* either dGTP or dTTP must be compared (Fig. 7). Discrimination is the ratio of the specificity constant (k_{pol}/K_d or k_{cat}/K_m) for the correct incorporation over that of the misincorporation. The resulting dimensionless number represents the magnitude of the preference for the correct nucleotide. A discrimination of 10,000 against 8-oxodGTP with respect to the direct competition with dGTP is lower than for most misincorporation events. However, the overall frequency of incorporating 8-oxodG can be reduced further by lowering the concentration of 8-oxodGTP in the mitochondria relative to that of dGTP. The concentrations of 8-oxodGTP in the mitochondria are not known, but the high concentrations of dGTP may lead to significant rates of oxidation to form 8-oxodGTP (33). This points to an important role for the triphosphatase, MutT homolog-1, in reducing the levels of 8-oxodGTP and thereby reducing rates of incorporation.

This is the first instance in which the slow pyrophosphate product release rate was shown to reduce k_{cat}/K_m , defining the nucleotide specificity constant (Fig. 3B). By allowing for the reversal of chemistry, the slow product release rate effectively reduces k_{cat}/K_m 3-fold according to the constants defined for 8-oxodG incorporation. Similarly, we have data showing that the chemistry step for AZT-triphosphate incorporation is

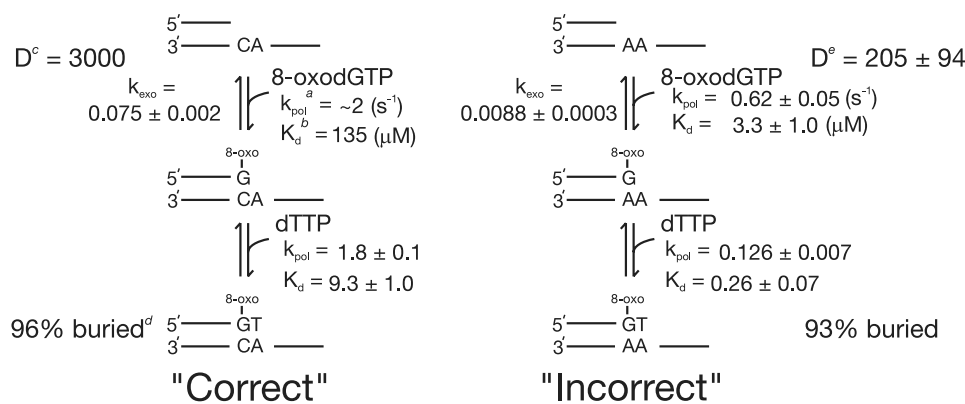


FIGURE 7. Overview of correct and incorrect incorporation of 8-oxodGTP kinetic parameters. The kinetic parameters obtained for the incorporation of 8-oxodGTP onto either dCMP (*Correct*) or dAMP (*Incorrect*) are shown *above*. In addition, other kinetic parameters such as the rate of excision and the incorporation of the next correct nucleotide are illustrated to the side of the corresponding step in the pathway. Most notable is a comparison of the values for the discrimination against 8-oxodGTP incorporation across from either dCMP or dAMP, respectively. This comparison predicts that the probability of incorrect incorporation is about 15-fold greater than that of the correct incorporation. Furthermore, the slow excision of 8-oxodGMP irrespective of template base suggests it is stably incorporated rather than removed for greater than 90% of events. ^a, the maximum rate of incorporation, k_{pol} , was estimated from the rate of the fast phase of incorporation at the highest concentration of 8-oxodGTP used. ^b, the K_d was determined using the program KinTekSim by global fitting to all the data for the incorporation of 8-oxodGTP onto dCMP simultaneously. ^c, a value of 3000 for the discrimination against 8-oxodGTP in the correct pathway was calculated as the ratio of correct dGTP incorporation determined previously (31) divided by the approximate specificity constant for 8-oxodGTP incorporation determined using the above values ($(k_{pol}/K_d)_{dGTP}/(k_{pol}/K_d)_{8-oxodGTP}$). ^d, the percent buried was calculated using Equation 5. ^e, the discrimination against 8-oxodGTP onto dAMP was calculated as in the correct pathway except that the specificity constant of dTTP incorporation was used ($(k_{pol}/K_d)_{dTTP}/(k_{pol}/K_d)_{8-oxodGTP}$).

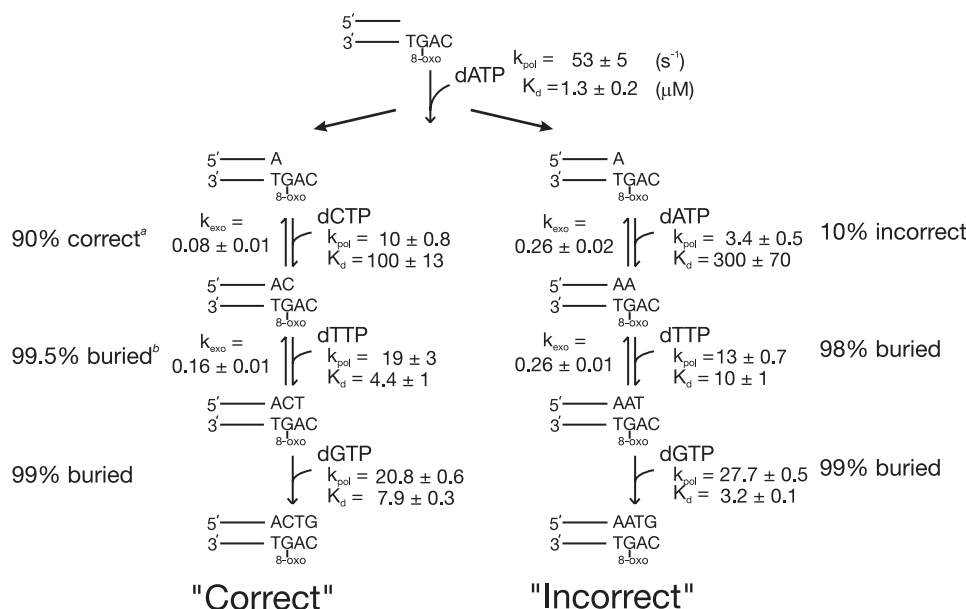


FIGURE 8. Overview of correct and incorrect pathways of polymerization with 8-oxodGMP present in the template strand. Shown in the *scheme* are the kinetic parameters that were obtained for each step of DNA synthesis for the two most likely routes (dCTP or dATP incorporation onto 8-oxodGMP). Depicted at the *top* of the *scheme* is the correct incorporation of dATP one base before 8-oxodGMP in the template strand. The branch point occurs when the polymerase either correctly incorporates dCTP (*left-hand pathway*) or incorrectly incorporates dATP (*right-hand pathway*). There is about a 90% probability that dCTP is chosen. The rates of excision are also shown for each of the steps, which allows for the calculation for the percent buried (next to the corresponding step). With respect to improving the fidelity of incorporation directly across from 8-oxodGTP, the proofreading exonuclease function is essentially negligible. ^a, determined using the ratio of the specificity constant for dCTP incorporation over that of dATP incorporation ($(k_{pol}/K_d)_{dCTP}/(k_{pol}/K_d)_{dATP}$). ^b, the percent buried was calculated using Equation 5.

reversible and pyrophosphate release is slow.³ This represents a novel mechanism by which a polymerase can increase discrimination against an undesirable substrate. Pyrophosphate release

³ J. Hanes and K. A. Johnson, manuscript in preparation.

is normally considered to be fast to account for fast processive synthesis. Examination of the kinetics processive synthesis reveals that each incorporation reaction proceeds at a rate approximately equal to the rate observed in a single turnover (28, 34). Therefore, there is no significant delay after the incorporation of one nucleotide and preceding the binding of the next. Steps involving pyrophosphate release and translocation are not well defined but must be faster than the rate of incorporation measured in a single turnover.

In the case of 8-oxodG and AZT, slow pyrophosphate release allows for the direct reversal of the chemistry step and reduces k_{cat} for incorporation. It is interesting to speculate that the mitochondrial polymerase evolved this method to reduce incorporation of 8-oxodG and that AZT may react in a similar way.

The vast majority of incorporation events go unnoticed by the proofreading exonuclease in that the probability of forward polymerization was much faster than the rates of excision for each base pair involving 8-oxodG. With respect to continuing replication, there is a surprisingly small effect resulting from the presence of 8-oxodGMP in the primer or template strand. Processive polymerization experiments were performed in the presence of a DNA trap to inspect the possibility that Pol γ may dissociate during replication if a damaged base is nearby. Pol γ efficiently copied 20 nucleotides beyond the damaged DNA site (to the end of the template strand) regardless of whether 8-oxodGMP was in the primer or template as well as correctly or incorrectly base paired (data not shown).

In Fig. 8 we summarize the kinetics of incorporation, excision, and extension with 8-oxodG in the template. The first step shown in the

pathway is dATP incorporation preceding the 8-oxodG in the template. This step is minimally affected when compared with the incorporation onto an undamaged DNA substrate (40 ± 7 versus $57 \pm 6 \mu\text{M}^{-1} \text{s}^{-1}$, respectively). The most affected incorporation event is the insertion of a nucleotide directly across

TABLE 1
Kinetic parameters for the incorporation of the dNTPs onto a template 8-oxodGMP

dNTP	k_{pol} s^{-1}	K_d μM	Specificity (k_{pol}/K_d)	Discrimination ^a
dCTP	10 ± 0.8	100 ± 13	0.100 ± 0.001	1
dATP	3.4 ± 0.5	300 ± 70	0.011 ± 0.003	9.1
dGTP	0.07 ± 0.01	550 ± 150	(1.3 ± 0.4) × 10 ⁻⁴	770
dTTP	(6.1 ± 0.5) × 10 ⁻³	110 ± 20	(5.5 ± 0.2) × 10 ⁻⁵	1800

^a Discrimination was calculated by the ratio of specificity constants for the correct incorporation (dCTP onto 8-oxodGMP) divided by that of each of the dNTPs ($(k_{\text{pol}}/K_d)_{\text{dCTP}}/(k_{\text{pol}}/K_d)_{\text{dNTP}}$).

from 8-oxodG. The specificity constant for dCMP incorporation across from 8-oxodGMP is reduced by about 470-fold (compared with incorporation onto undamaged DNA) but is sufficiently fast for the polymerase to continue replication without dissociation from the duplex. However, the fidelity of replication is reduced significantly. Discrimination against the formation of the undamaged DNA mispair, dA:dG, is 280,000 ± 80,000 (30), but the discrimination is reduced to 9 ± 0.3 (more than 30,000-fold) for the dA:8-oxodG mispair. Pol γ discriminates relatively poorly against the incorporation of dGTP and dTTP onto 8-oxodGMP, with values for discrimination of 770 ± 240 and 1820 ± 70, respectively (Table 1).

Overall, 8-oxodGMP in the template DNA strand dramatically reduces the fidelity of incorporation, coding for dAMP about 1/10 incorporation events. The enzyme is able to continue polymerization over 8-oxodG without dissociation, and the proofreading exonuclease activity is not effective at correcting the mismatch with dAMP. The incorporation of 8-oxodGTP appears to be especially mutagenic compared with 8-oxodG in the template. During the course of one's life, this lack of discrimination against both the formation of dA:8-oxodG and 8-oxodG:dA mispairs along with inefficient proofreading by Pol γ may contribute to the complicated process of aging and to the cumulative toxic side effects of nucleoside analogs used to treat human immunodeficiency virus infections, which are thought to be compounded by increased oxidative stress resulting from impaired mitochondrial DNA replication (25).

REFERENCES

- Loeb, L. A., Wallace, D. C., and Martin, G. M. (2005) *Proc. Natl. Acad. Sci. U. S. A.* **102**, 18769–18770
- Dufour, E., and Larsson, N. G. (2004) *Biochim. Biophys. Acta* **1658**, 122–132
- Shigenaga, M. K., Hagen, T. M., and Ames, B. N. (1994) *Proc. Natl. Acad. Sci. U. S. A.* **91**, 10771–10778
- Barja, G. (2004) *Trends Neurosci.* **27**, 595–600
- Alexeyev, M. F., Ledoux, S. P., and Wilson, G. L. (2004) *Clin. Sci. (Lond.)* **107**, 355–364

- Gao, D., Wei, C., Chen, L., Huang, J., Yang, S., and Diehl, A. M. (2004) *Am. J. Physiol. Gastrointest. Liver Physiol.* **287**, 1070–1077
- Herrero, A., and Barja, G. (1999) *Aging (Milano)* **11**, 294–300
- Souza-Pinto, N. C., Hogue, B. A., and Bohr, V. A. (2001) *Free Radic. Biol. Med.* **30**, 916–923
- Stevnsner, T., Thorslund, T., Souza-Pinto, N. C., and Bohr, V. A. (2002) *Exp. Gerontol.* **37**, 1189–1196
- Kamiya, H. (2003) *Nucleic Acids Res.* **31**, 517–531
- Sakumi, K., Furuichi, M., Tsuzuki, T., Kakuma, T., Kawabata, S., Maki, H., and Sekiguchi, M. (1993) *J. Biol. Chem.* **268**, 23524–23530
- Yoshimura, D., Sakumi, K., Ohno, M., Sakai, Y., Furuichi, M., Iwai, S., and Nakabeppu, Y. (2003) *J. Biol. Chem.* **278**, 37965–37973
- Kang, D., Nishida, J., Iyama, A., Nakabeppu, Y., Furuichi, M., Fujiwara, T., Sekiguchi, M., and Takeshige, K. (1995) *J. Biol. Chem.* **270**, 14659–14665
- Larsen, N. B., Rasmussen, M., and Rasmussen, L. J. (2005) *Mitochondrion* **5**, 89–108
- Einolf, H. J., Schnetz-Boutaud, N., and Guengerich, F. P. (1998) *Biochemistry* **37**, 13300–13312
- Einolf, H. J., and Guengerich, F. P. (2001) *J. Biol. Chem.* **276**, 3764–3771
- Pinz, K. G., Shibutani, S., and Bogenhagen, D. F. (1995) *J. Biol. Chem.* **270**, 9202–9206
- Shibutani, S., Takeshita, M., and Grollman, A. P. (1991) *Nature* **349**, 431–434
- Gannett, P. M., and Sura, T. P. (1993) *Chem. Res. Toxicol.* **6**, 690–700
- Krahn, J. M., Beard, W. A., Miller, H., Grollman, A. P., and Wilson, S. H. (2003) *Structure (Camb)* **11**, 121–127
- Trifunovic, A., Wredenberg, A., Falkenberg, M., Spelbrink, J. N., Rovio, A. T., Bruder, C. E., Bohlooly, Y., Gidlof, S., Oldfors, A., Wibom, R., Tornell, J., Jacobs, H. T., and Larsson, N. G. (2004) *Nature* **429**, 417–423
- Kujoth, G. C., Hiona, A., Pugh, T. D., Someya, S., Panzer, K., Wohlgemuth, S. E., Hofer, T., Seo, A. Y., Sullivan, R., Jobling, W. A., Morrow, J. D., Van Remmen, H., Sedivy, J. M., Yamasoba, T., Tanokura, M., Weindruch, R., Leeuwenburgh, C., and Prolla, T. A. (2005) *Science* **309**, 481–484
- Schriner, S. E., Linford, N. J., Martin, G. M., Treuting, P., Ogburn, C. E., Emond, M., Coskun, P. E., Ladiges, W., Wolf, N., Van Remmen, H., Wallace, D. C., and Rabinovitch, P. S. (2005) *Science* **308**, 1909–1911
- Lee, H., Hanes, J., and Johnson, K. A. (2003) *Biochemistry* **42**, 14711–14719
- Lewis, W., Copeland, W. C., and Day, B. J. (2001) *Lab. Investig.* **81**, 777–790
- Graves, S. W., Johnson, A. A., and Johnson, K. A. (1998) *Biochemistry* **37**, 6050–6058
- Johnson, A. A., Tsai, Y., Graves, S. W., and Johnson, K. A. (2000) *Biochemistry* **39**, 1702–1708
- Patel, S. S., Wong, I., and Johnson, K. A. (1991) *Biochemistry* **30**, 511–525
- Donlin, M. J., Patel, S. S., and Johnson, K. A. (1991) *Biochemistry* **30**, 538–546
- Lee, H. R., and Johnson, K. A. (2006) *J. Biol. Chem.* **281**, 36236–36240
- Johnson, A. A., and Johnson, K. A. (2001) *J. Biol. Chem.* **276**, 38090–38096
- Tsai, Y. C., and Johnson, K. A. (2006) *Biochemistry* **45**, 9675–9687
- Mathews, C. K. (2006) *FASEB J.* **20**, 1300–1314
- Kati, W. M., Johnson, K. A., Jerva, L. F., and Anderson, K. S. (1992) *J. Biol. Chem.* **267**, 25988–25997